Expression and characterization of *Pseudomonas aeruginosa* cytochrome *c*-551 and two site-directed mutants: role of tryptophan 56 in the modulation of redox properties

Francesca CUTRUZZOLÀ*§, Ilaria CIABATTI*‖, Gabriella ROLLI*, Sabrina FALCINELLI*, Marzia ARESE*, Graziella RANGHINO†, Andrea ANSELMINO†, Elisabetta ZENNARO‡ and Maria Chiara SILVESTRINI*

*Istituto Pasteur-Fondazione Cenci-Bolognetti, Dipartimento di Scienze Biochimiche A. Rossi Fanelli, Università di Roma La Sapienza, 00185 Roma, Italia, †EniChem, Istituto Guido Donegani, Novara, Italia, ‡Dipartimento di Biologia Cellulare e dello Sviluppo, Università di Roma La Sapienza, Roma, Italia

The gene coding for *Pseudomonas aeruginosa* cytochrome *c*-551 was expressed in *Pseudomonas putida* under aerobic conditions, using two different expression vectors; the more efficient proved to be pNM185, induced by *m*-toluate. Mature holo-(cytochrome *c*-551) was produced in high yield by this expression system, and was purified to homogeneity. Comparison of the recombinant wild-type protein with that purified from *Ps. aeruginosa* showed no differences in structural and functional properties. Trp^{56}, an internal residue in cytochrome *c*-551, is located at hydrogen-bonding distance from haem propionate-17, together with Arg^{47}. Ionization of propionate-17 was related to the observed pH-dependence of redox potential. The role of Trp^{56} in determining the redox properties of *Ps. aeruginosa* cytochrome *c*-551 was assessed by site-directed mutagenesis, by substitution with Tyr (W56Y) and Phe (W56F). The W56Y mutant is similar to the wild-type cytochrome. On the other hand, the W56F mutant, although similar to the wild-type protein in spectral properties and electron donation to azurin, is characterized by a weakening of the Fe–Met^{61} bond, as shown in the oxidized protein by the loss of the 695 nm band approx. 2 pH units below the wild-type. Moreover, in W56F, the midpoint potential and its pH-dependence are both different from the wild-type. These results are consistent with the hypothesis that hydrogen-bonding to haem propionate-17 is important in modulation of the redox properties of *Ps. aeruginosa* cytochrome *c*-551.

INTRODUCTION

The *c* cytochromes are probably the most studied electron-transfer (ET) proteins, in all possible respects, ranging from primary, secondary and tertiary structure, in the crystal and in solution, to thorough physicochemical, biochemical and kinetic characterization of native and chemically modified forms [1]. Recently, additional information has become accessible through cloning, sequencing and expression of genes, with synthesis of site-directed mutants [2]. These investigations are aimed at understanding the mechanisms whereby the protein matrix controls the redox potential of the prosthetic group and the specificity and rates of ET. This goal, probably closer for cytochrome *c* than for any other protein, is as yet elusive. Further implications may be envisaged in the elucidation of physiologically relevant processes such as pH modulation of redox potential in respiratory membrane or in bacterial periplasm.

In *c* cytochromes, the prosthetic group protohaem IX is bound to the protein via thioether bonds between two cysteine residues and the two vinyl substituents of the protoporphyrin ring, with the iron ion co-ordinated to the protein via at least one His. All *c* cytochromes of known sequence share the Cys-X-Y-Cys-His haem attachment site and most of them have been grouped on the basis of sequence homology, tertiary structure, redox potential and spectroscopic features into four major classes [1].

Cytochrome *c*-551 from *Ps. aeruginosa* (referred to from now on as *c*-551) is a monomeric redox protein of 82 amino acid residues [3], involved in the bacterial denitrification chain, where it donates electrons to nitrite reductase and possibly interacts with azurin [4]. The three-dimensional structure of *Ps. aeruginosa* *c*-551 has been solved at high resolution by both X-ray crystallography [5] and NMR [6]. It is a member of the bacterial class I cytochromes; a strong sequence homology is present among *c*-551 from several species (also called cytochromes c_7 [1]). The bacterial proteins in this class share with mitochondrial class-I cytochromes common features such as: (i) a single hexa-co-ordinated low-spin haem; (ii) a Met residue as the sixth haem axial ligand, yielding in the oxidized protein an absorption band at 695 nm, and located in the sequence a long way from the proximal ligand His; (iii) a high α-helical content; (iv) characteristic polypeptide folding around the haem, which leaves the edges of pyrrole rings II and III exposed. One of the main structural differences between mitochondrial and bacterial class-I *c* cytochromes lies in the fact that the latter are smaller, lacking a loop around the haem. This causes further exposure of the haem edge, especially at the level of propionate 13 (HP-13; recommended IUB-IUPAC nomenclature).

The functional properties of *Ps. aeruginosa* *c*-551 have been extensively investigated, in reactions with both non-physiological small inorganic redox reactants [7] and other macromolecules, such as blue copper proteins [8,9], eukaryotic cytochrome *c* [10]

Abbreviations used: *c*-551, cytochrome c_{551}; HP, haem propionate; ESMS, electron-spray mass spectrometry; ET, electron transfer; MD, molecular dynamics; IPTG, isopropyl β-D-thiogalactopyranoside.

§ To whom correspondence should be addressed.

‖ Present address: Istituto Zooprofilattico Sperimentale delle Regioni Lazio e Toscana, Roma, Italia.

and the physiological partner, nitrite reductase [11,12]. The self-exchange rate, a critical parameter in the framework of the Marcus theory for ET reactions [13], was found to be high ($k = 10^7\ M^{-1} \cdot s^{-1}$ [14]). *Ps. aeruginosa* *c*-551 is located in the bacterial periplasm; it is synthesized as a precursor protein of 104 amino acids, with a signal peptide of 22 amino acids, starting from a single gene (*nirM*) located in a larger operon which also contains the gene coding for nitrite reductase (*nirS*). The *nirM* gene has been isolated and sequenced [15,16].

As a necessary step towards protein engineering of *c*-551, the *nirM* gene of *Ps. aeruginosa* was isolated, and the protein expressed in the heterologous system of *Ps. putida*. The efficient expression system and a new purification method guarantee high yields of the recombinant protein. A thorough characterization of this protein shows that it is indistinguishable from the native *c*-551 purified from *Ps. aeruginosa*. In order to investigate the influence of strategically located residues on the redox properties of *c*-551, we focused our attention on the Trp at position 56. This residue is highly conserved in all *c*-551 (except in *Rhodocyclus gelatinosa* [17], where it is replaced by a Phe). An homologous Trp is also highly conserved in other class-I *c* cytochromes (Trp^{64} in *Saccharomyces cerevisiae* iso-1-cytochrome *c*, Trp^{59} in horse heart cytochrome *c*, Trp^{67} in *Rhodobacter capsulatus* cytochrome c_2) [1]. In *Ps aeruginosa* *c*-551 Trp^{56} is located, together with Arg^{47}, at hydrogen-bonding distance from haem propionate-17 (HP-17) [5], the ionization of which has been proposed to be related to the observed pH-dependence of redox potential [18]; in eukaryotic cytochrome *c* little pH-dependence has been observed between pH 4.5 and 9.0. Whereas some information on the role of residue 47 is available from the comparison with *Pseudomonas stutzeri* *c*-551 [19] where this position is occupied by His, the role of Trp^{56} in *c*-551 was not yet investigated. We have prepared two site-directed mutants in which Trp^{56} has been replaced by Phe (W56F) and Tyr (W56Y) and analysed several physicochemical properties of these proteins, including their interaction with azurin.

EXPERIMENTAL

Bacterial strains and growth

Escherichia coli HB101 was the host strain for plasmid manipulations. *Ps. putida* strain PaW340, a plasmid free St^R, Trp^- mutant of mt2, was grown at 30 °C, in Luria–Bertani liquid medium. When appropriate, antibiotics were added at the following concentrations (μg/ml): ampicillin 100, kanamycin 30, tetracycline 25. Cultures were grown in the presence of 5 mM *m*-toluate when required for induction of the Pm promoter or in the presence of 1 mM isopropyl β-D-thiogalactopyranoside (IPTG) in the case of the *lac* promoter.

Plasmids and recombinant DNA techniques

All DNA manipulations were performed by following standard protocols. The construction of plasmids pEMBL18-NR and pNM-NR was as previously described [20,21]. These plasmids harbour a 3.5 kb *Eco*RI fragment containing *nirS* [20] and *nirM* [15,16] genes from *Ps. aeruginosa*, the restriction map of which is reported in Figure 1(A). The plasmid pNM185 [22] used for expression is a broad-host-range vector containing: (i) the positively activated Pm promoter of the TOL plasmid upstream of the streptomycin-resistance (Sm^R) gene; (ii) the *xylS* gene, which codes for the positive regulator of Pm; (iii) the kanamycin-resistance (Km^R) gene as selectable marker. Transcription from the Pm promoter is activated by the *xylS* gene product in the presence of *m*-toluate [23]. The plasmid pME3814 is an expression vector containing the *lac* promoter. The plasmids pTZ18R and pTZ19R are multifunctional phagemids (Pharmacia Biotech). Transformation of *Ps. putida* PaW340 was performed as described by Lederberg and Cohen [24]. The oligonucleotides used for *nirM* gene subcloning by PCR were:

5′-CGGCGC<u>GAATTC</u>**GAGGAACCGTG**<u>**ATG**</u>**AAACCGTA-CGCACTGC**-3′ (1)

*Eco*RI RBS Met

5′-CGGCGC<u>GAATTC</u>**TCA**TTTCTGCGACAGGACCCACT-**TCGCC**-3′ (2)

*Eco*RI End

5′-CGGCGC<u>GAATTC</u>**ATG**AAACCGTACGCACTGCTTTC-**GCTGC**-3′ (3)

*Eco*RI Met

5′-CGGCGC<u>GGATCC</u>**TCA**TTTCTGCGACAGGACCCACT-**TCGCC**-3′ (4)

*Bam*HI End

Oligonucleotides 1 and 3 are identical to the *nirM* gene coding sequence (bold characters), from the initial Met codon; their sequence was designed to insert an *Eco*RI site (underlined) at the 5′ end of the sequence to be amplified and, for primer 1, the ribosome-binding site (RBS). The sequences of oligonucleotides 2 and 4 are the reverse complement of the coding strand of the *nirM* gene (bold characters), starting from the stop codon; their sequence allowed the insertion of an *Eco*RI and a *Bam*HI site (underlined) at the 3′ end of the sequence to be amplified. PCR was carried out on a Perkin–Elmer 480 thermal reactor, with a hybridization temperature of 58 °C for 30 cycles, using Amplitaq DNA polymerase (Perkin–Elmer Cetus). The fragment amplified using as primers oligonucleotides 1 and 2 was cloned into the *Eco*RI site of pNM185 and that amplified with primers 3 and 4 was cloned into pME3814, yielding the recombinant plasmids pNM*cyt* and pME*cyt* respectively. The amplified fragments were also cloned into pTZ18R and pTZ19R for dideoxy-DNA sequencing carried out using Sequenase 2.0 reagents (US Biochemicals). Mutagenesis of the *nirM* gene was performed by the double-strand plasmid method of Inouye and Inouye [25] starting from the plasmids pTZ18R and pTZ*cyt* (containing the gene amplified with oligonucleotides 1 and 2). The degenerate oligonucleotide used to obtain mutants W56F and W56Y was:

5′-CGTTCGGCGGCATCGGGATCGGGCCG**A**(**T**)AGACG-CCCTGGC-3′

Screening of the mutants was carried out by restriction analysis, since the mutation also leads to loss of a unique *Apa*I site, and confirmed by sequencing the entire gene. Subcloning of the mutated genes into the *Eco*RI site of the expression vector pNM185 was performed as described for the wild-type gene (see above).

Recombinant *c*-551 purification

For protein purification, the *Ps. putida* PaW340 strain containing the appropriate plasmid was grown at 30 °C in a 50 litre fermentor under induction conditions. The wet cell paste was resuspended in 20 mM sodium phosphate buffer, pH 7.0, containing 1 mM PMSF and 1 mM EDTA (8 ml/g wet weight), sonicated and fractionated with $(NH_4)_2SO_4$ at 40 and 70% saturation. These steps were followed by a DEAE-cellulose batchwise treatment in 20 mM sodium phosphate buffer, pH 7.0, as described by Parr et

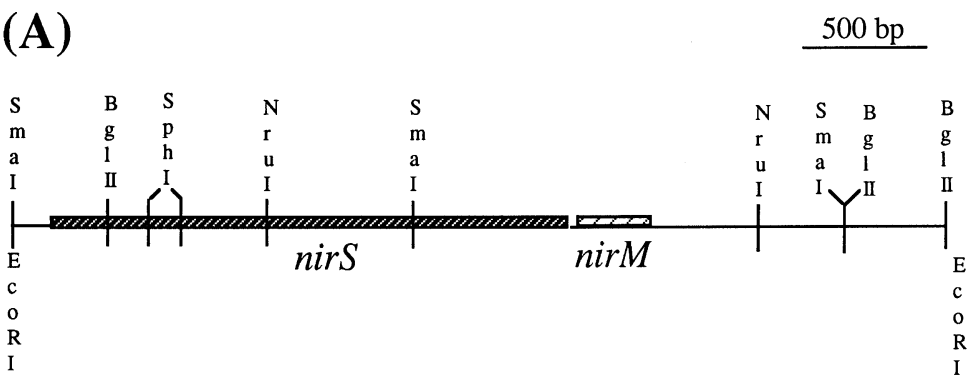

(B)

```
ATGAAACCGTACGCACTGCTTTCGCTGCTCGCCACCGGCACCCTGCTCGCCCAGGGCGCC
---------+---------+---------+---------+---------+---------+ 60
TACTTTGGCATGCGTGACGAAAGCGACGAGCGGTGGCCGTGGGACGAGCGGGTCCCGCGG

M  K  P  Y  A  L  L  S  L  L  A  T  G  T  L  L  A  Q  G  A

TGGGCCGAAGACCCCGAAGTGCTGTTCAAGAACAAGGGCTGCGTGGCCTGCCATGCCATC
---------+---------+---------+---------+---------+---------+ 120
ACCCGGCTTCTGGGGCTTCACGACAAGTTCTTGTTCCCGACGCACCGGACGGTACGGTAG

W  A  E  D  P  E  V  L  F  K  N  K  G  C  V  A  C  H  A  I

GACACCAAGATGGTCGGCCCGGCCTACAAGGACGTCGCCGCCAAGTTCGCCGGCCAGGCC
---------+---------+---------+---------+---------+---------+ 180
CTGTGGTTCTACCAGCCGGGCCGGATGTTCCTGCAGCGGCGGTTCAAGCGGCCGGTCCGG

D  T  K  M  V  G  P  A  Y  K  D  V  A  A  K  F  A  G  Q  A

GGCGCGGAAGCGGAACTCGCGCAGCGGATCAAGAACGGCAGCCAGGGCGTCTGGGGCCCG
---------+---------+---------+---------+---------+---------+ 240
CCGCGCCTTCGCCTTGAGCGCGTCGCCTAGTTCTTGCCGTCGGTCCCGCAGACCCCGGGC

G  A  E  A  E  L  A  Q  R  I  K  N  G  S  Q  G  V  W  G  P

ATCCCGATGCCGCCGAACGCGGTCAGCGACGACGAGGCGCAGACCCTGGCGAAGTGGGTC
---------+---------+---------+---------+---------+---------+ 300
TAGGGCTACGGCGGCTTGCGCCAGTCGCTGCTGCTCCGCGTCTGGGACCGCTTCACCCAG

I  P  M  P  P  N  A  V  S  D  D  E  A  Q  T  L  A  K  W  V

CTGTCGCAGAAATGA
---------+----- 315
GACAGCGTCTTTACT

L  S  Q  K  *
```

Figure 1 Localization and sequence of the *nirM* gene from *Ps. aeruginosa*

(**A**) Restriction map of the 3.5 kb fragment, showing the location of *nirS* and *nirM* genes. (**B**) Nucleotide sequence of the *nirM* gene and the derived amino acid sequence. The site of the difference found with respect to other *nirM* genes (see the text) is underlined.

al. [26]. The majority of contaminant proteins were then eliminated by taking the sample to pH 3.9 by the addition of acetic acid. The last purification step was a CM-Sepharose ion-exchange chromatography as in [26]. SDS/Tricine/PAGE [27] was carried out at several stages of the purification procedure and the presence of haem was detected using the method of Thomas et al. [28].

Protein sequencing was carried out on purified recombinant cytochrome loaded on a gas-phase sequencer (Applied Biosystems model 470A) equipped with a phenylthiohydantoin analyser (model 120A). M_r values of wild-type and recombinant *c*-551 were determined by electron-spray mass spectrometry (ESMS) on a single-quadrupole HP5989A MS-Engine spectrometer (Hewlett–Packard). The instrument was calibrated with a myoglobin standard solution.

Spectroscopy

Spectrophotometric measurements were carried out on a Cary 219 or on a Jasco V500 spectrophotometer. Different titrations

were measured at 20 °C. (1) For titration of the 551 nm band, cytochromes were dialysed overnight against 50 mM ammonium acetate, pH 5.7, and a 5–6 μM protein solution, reduced with 10 mM ascorbic acid, was titrated by sequential additions of 10 M NaOH. (2) For titration of the 695 nm band, cytochromes were dialysed overnight against 50 mM ammonium acetate, pH 6.5, and a 100 μM solution of oxidized protein was titrated by sequential additions of 10 M NaOH. CD measurements were recorded in the visible and UV regions at 20 °C with a Jasco J500 spectropolarimeter, equipped with a Jasco model DP 500 N data processor.

Kinetics of the reaction between reduced *c*-551 and excess oxidized azurin were measured with an Applied Photophysics (UK) DX.17MV stopped-flow apparatus at 25 °C in 0.1 M sodium phosphate buffer, pH 7.0, as previously described [8]. Reduced *c*-551 was prepared by the addition of sodium dithionite, followed by Sephadex G-25 chromatography to remove dithionite oxidation products. The observed kinetic process under pseudo-first-order conditions was analysed as a simple exponential. Equilibrium constants were determined by spectrophotometric titrations of reduced *c*-551 with oxidized azurin under the conditions used for kinetic measurements [9].

Redox potential measurements

Midpoint oxidation–reduction (redox) potentials were determined spectrophotometrically for each cytochrome in the presence of a ferricyanide–ferrocyanide solution of known potential [29]. This method allows a single potential measurement to be made at a defined pH. For each redox potential measurement the ferrocyanide concentration was 0.5 mM and additions of ferricyanide (0.0, 0.003 and 0.017 mM) were made; the cytochrome concentration was 5–6 μM. The redox mixture was buffered at a chosen pH value by the addition of 2 mM acetic acid/sodium acetate, pH 4.5–5.8, 2 mM sodium phosphate, pH 5.8–7.5, 2 mM Tris/HCl, pH 7.5–8.8 and 2 mM sodium borate/NaOH, pH 9–10.7. The measurements were made at 20 °C.

Molecular modelling

Co-ordinates from the crystal structure at 1.6 Å (0.16 nm) resolution of oxidized native *c*-551 were used (PDB entry 451C). Molecules were soaked in a water environment to simulate their behaviour in solution by adding a 9 Å-thick layer in the 'water droplet' cluster approach. Hydrogen atoms were added and energy minimization of 500–1000 steps was performed by the conjugate-gradient method, for both the native and mutant proteins; in this step a tethering of 100/50 kcal/Å^2 was imposed on backbone atoms in order to prevent excessive modification of the three-dimensional structure. After the minimization, the dynamic behaviour of the proteins was simulated by a molecular dynamic (MD) cycle at room temperature. The first 5 ps of the simulation constitute the heating and equilibration phases. Dynamics simulations last 100 ps altogether, at a temperature of 300 K. As a precaution against instability from inadequate equilibration, not only the 3 ps of the initializing phase, but also some of the first picoseconds of the trajectories are not included in the analysis. The average conformation of the atomic positions over the last 10 ps of the simulation is considered to be the resulting average conformation of the molecule. All MD procedures were performed using software programs from Biosym Technologies (dynamics with DISCOVER and graphical display with INSIGHT II). The consistent valence force field provided by DISCOVER is used with the force field reported by Angelucci et al. [30] for the atom pairs including iron.

The software GREENPATH [31,32] was used to compute the electronic coupling between an atom that either donates or accepts an electron and all other atoms in the same molecule. The program also gives the value of coupling for a residue with respect to its distance from the donor; this quantity is computed as the ratio between effective coupling provided by the GREENPATH model and a value for the coupling provided by the only distance model with exponential decay and constant parameters [coupling = $const \exp(-1.4\ R)$, where R is the distance between the redox centres and *const* is a constant]. GREENPATH is used also to evaluate all physical tunnelling pathways between two points of the same protein in the case of intramolecular ET, or between an electron source into a molecule and an acceptor centre into another molecule in the case of intermolecular ET.

RESULTS

c-551 gene cloning and expression

On the basis of the isolation and sequencing of *Ps. aeruginosa c*-551 gene (*nirM* gene) reported in the literature [15,16], we have located, by nucleotide sequencing, the *nirM* gene in the 3.5 kb genomic DNA fragment previously isolated [20], which also contains the gene coding for nitrite reductase (*nirS* gene). Figure 1 shows the 3.5 kb fragment map with the location of the two genes (Figure 1A) and the nucleotide sequence of the *nirM* gene and its translation product (Figure 1B).

Ps. aeruginosa c-551 was initially expressed in *Ps. putida* starting from the pNM-NR recombinant plasmid [21], containing the entire 3.5 kb fragment in the *Eco*RI site of the vector pNM185. To optimize protein expression, which in the framework of the operon is relatively low and results in complex protocols for large-scale growth and protein purification, we isolated the *nirM* gene by PCR and subcloned it into two different expression vectors, yielding the recombinant plasmids pNM*cyt* and pME*cyt*, as described in the Experimental section. The nucleotide sequence of the amplified DNA that resulted was identical with that previously published for the *nirM* gene [15,16], except at position 102 of the coding sequence, where a T to C silent substitution was found (Figure 1). This difference, which was also confirmed by sequencing the chromosomal gene, may be due to the fact that the *Ps. aeruginosa* strain we used for genomic DNA isolation [20] is different from that of Arai et al. [16] and Nordling et al. [15].

Ps. putida strain PaW340 was transformed with the recombinant plasmids pNM*cyt* and pME*cyt*, and expression was induced by addition of 5 mM *m*-toluate or 1 mM IPTG respectively. *c*-551 was indeed produced and matured correctly in both expression systems, but the pNM*cyt*-containing strain gave a higher yield of recombinant protein. Thus the following characterization refers to the protein purified from pNM*cyt*-transformed cells.

Characterization of wild-type recombinant *c*-551

The recombinant *c*-551 was purified by the novel procedure described in the Experimental section with a yield of 0.5 mg/g wet weight of cells. It migrates as a single band on SDS/Tricine/PAGE consistent with its M_r, and has a covalently linked haem, as observed by haem-specific gel staining [28] (not shown). N-Terminal sequencing of the protein for 31 cycles shows the sequence expected for the mature protein after proteolytic cleavage of the signal peptide. The M_r of the recombinant protein, determined by ESMS, was 9308.9, which is identical with that of the native protein from *Ps. aeruginosa*

Table 1 p*K* values of relevant transitions in *c*-551

Values are means ± S.E.M. Column 1 gives p*K* of the alkaline transition involving the spectral band at 695 nm in the oxidized protein; columns 2 and 3 give p*K* of the transition involving the spectral band at 551 nm in the reduced protein; columns 4 and 5 give p*K* calculated from ferricyanide redox titrations of *c*-551 using eqn (1). n.d., not determined.

c-551	pK_{695}	pK_{red551} ($I = 50$ mM)	pK_{red551} ($I = 6$ mM)	pK_{red} ($I = 2$ mM)	pK_{ox} ($I = 2$ mM)
Ps. aeruginosa	11.0 ± 0.2	7.1 ± 0.1	n.d.	7.6	6.5
Recombinant	11.0 ± 0.2	7.1 ± 0.1	n.d.	7.7	6.6
W56Y	10.7 ± 0.2	6.8 ± 0.2	6.7 ± 0.1	7.5	6.6
W56F	9.4 ± 0.2	8.6 ± 0.4	9.8 ± 0.1	10.4	6.5

(9309). The optical properties (visible and UV absorption and CD spectra) of the purified recombinant *c*-551 are identical in both oxidation states with those described previously for the native protein [4,33] (not shown). Moreover, the shape and intensity of the α-band in the reduced form show the pH-dependence characteristic of *Ps. aeruginosa* *c*-551 with a p*K* of approx. 7 (Table 1) [9,34]. Several other functional and structural properties of recombinant *c*-551 have been investigated and are discussed below in parallel with the properties of W56F and W56Y mutants.

Production and characterization of the W56F and W56Y mutants

Mutagenesis of the *nirM* gene was performed by the double-strand plasmid method of Inouye and Inouye [25] and confirmed by sequencing the entire gene. Expression and purification of the W56F and W56Y mutants was achieved by the strategy outlined for the wild-type *c*-551, using the vector pNM185 and *Ps. putida* as a host strain, with comparable yields of purified protein. The M_r of W56F and W56Y was also determined by ESMS, yielding values of 9269.8 and 9285.8 respectively, which confirmed the M_r differences expected for the Trp → Phe (−39) and Tyr (−23) mutations.

The absorption spectra of the mutant proteins are identical with that of the wild-type in both redox states, with the exception of the 250–300 nm region where, as expected for the Trp → Phe or Tyr mutations, a decrease in absorption is observed compared with the wild-type (not shown). The CD spectra of the W56F and W56Y are also superimposable on the wild-type spectra; in particular, the region between 200 and 250 nm, diagnostic of the secondary structure, shows that the α-helical content is well conserved in the mutants (results not shown).

The presence of a 695 nm band in the absorption spectrum of many *c* ferric cytochromes is a diagnostic feature of ligation of the low-spin Fe(III) with the bivalent sulphur of the axial ligand Met. This band is lost under several conditions, such as extreme pHs, high temperature or presence of denaturants, and its disappearance has been related to Met displacement by other internal ligands, such as Lys^{79} in yeast iso-1-ferricytochrome *c* [35]. The alkaline p*K* of this 695 nm transition lies between pH 8 and 11 in various proteins [1]; mitochondrial cytochromes usually have a value centred around 9, whereas in *Ps. aeruginosa* *c*-551 the 695 nm band transition has a p*K* of 11. In order to test the features of the Met–Fe bond in the recombinant wild-type and mutant proteins, the 695 nm band was followed by titrations at alkaline pH: the wild-type and W56Y mutant show an alkaline p*K* of 11.0 and 10.7 respectively, whereas the same transition in the W56F mutant displays a lower p*K* (9.4) (Table 1) showing that displacement of the Met ligand occurs in this mutant at a lower pH. The stereochemistry of the Met residue in both mutants appears to be conserved with respect to the wild-type, since the sign and amplitude of the CD signal in the region of the 695 nm band for the oxidized mutants are consistent with that observed for the wild-type *c*-551 [36] and opposite to that observed for horse heart cytochrome *c* (results not shown).

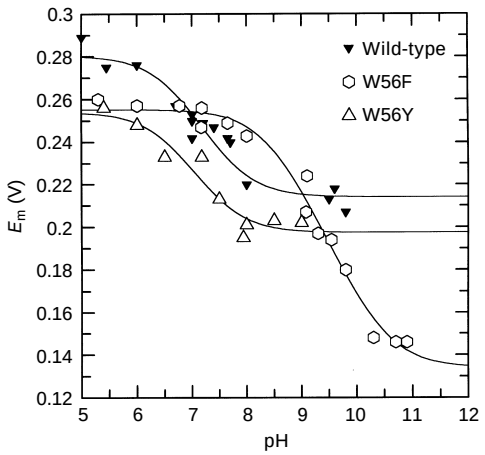

Figure 2 pH-dependence of the redox potential of recombinant *c*-551 (▼) and W56F (⬡) and W56Y (△) mutants

The redox potential of ET proteins often displays a pH-dependence that reflects the ionization of a single group [1]. In *Ps. aeruginosa* and *Ps. stutzeri* *c*-551, this group was identified with HP-17, which displays different p*K* values in the oxidized (pK_{ox}) and reduced (pK_{red}) states [18]. An estimate of the propionate p*K* can be obtained by studying the pH-dependence of the midpoint potential and, in *Ps. aeruginosa*, by optical titration of the α-band, which is red-shifted by the ionization [9,34]. An important role in the modulation of this transition has been assigned to residue 47 (Arg in *Ps. aeruginosa* and His in *Ps. stutzeri*) which partially or completely exchanges a proton with the HP-17 carboxylate [18,19]. Less studied is the role of Trp^{56}, which is also located at hydrogen-bonding distance from HP-17; we therefore measured the redox potential of the mutants W56F and W56Y as a function of pH in the presence of a ferricyanide–ferrocyanide couple of known potential. The data were analysed according to eqn (1):

$$E_m = E^* - 0.06 \log (K_{ox} + [H^+])/(K_{red} + [H^+]) \quad (1)$$

The results are shown in Figure 2 in comparison with the wild-type *c*-551: the values of pK_{red} and pK_{ox} obtained for the wild-type protein (Table 1) are in reasonable agreement with those previously determined for the native *Ps. aeruginosa* protein under the same experimental conditions [18]. The profile of midpoint potentials as a function of pH is rather different for the W56F mutant with respect to the unmutated protein. The pK_{red} shifts to higher values (approx. 10) as compared with the values of approx. 7.5 observed for the wild-type and W56Y (Table 1). Moreover, the absolute values of redox potential for W56F are lowered with respect to the wild-type, the greater decrease (80 mV) being at alkaline pH (Figure 2). In the case of the W56Y protein the observed redox potential is approx. 20 mV lower than wild-type over the whole pH range analysed. The p*K* of ferrocytochrome *c*-551 was also independently measured by optical pH titrations of the α-band at 551 nm [34] at two different ionic strengths ($I = 6$ and 50 mM). The values obtained (pK_{red551}, Table 1) show the same trend of the pK_{red} values as calculated

Table 2 Equilibrium and second-order rate constants for the reaction between oxidized wild-type azurin and reduced wild-type and mutant *c*-551 in 0.1 M phosphate buffer, pH 7.0, at 25 °C

K_{eq} values are means ± S.E.M. Errors in k_{12} values are about ± 10%.

c-551	K_{eq}	$10^{-6} \times k_{12}$ ($M^{-1} \cdot s^{-1}$)
Ps. aeruginosa	4.0 ± 0.5	9.0
Recombinant	4.5 ± 0.8	6.4
W56Y	10.5 ± 0.8	9.4
W56F	3.7 ± 0.5	8.2

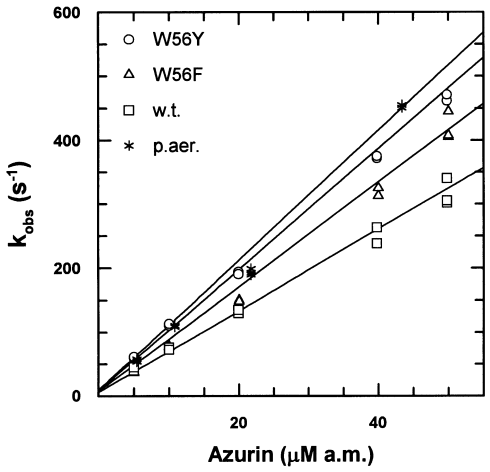

Figure 3 ET reaction between reduced *c*-551 and oxidized azurin

Dependence of the pseudo-first-order rate constant of the reaction on the concentration of oxidized azurin (after mixing). Experimental conditions: reduced *c*-551 was 2 μM in all cases; observations were carried out at pH 7.0; $\lambda = 417$ nm; 25 °C. Lines represent linear regressions of experimental data. w.t., wild-type; p. aer, *Ps. aeruginosa*.

from the analysis of the pH-dependence of the redox potential (i.e. a significantly higher p*K* for the W56F mutant); however, the absolute values are systematically lower, especially at the higher ionic strength explored.

The intermolecular ET reaction from reduced *c*-551 to oxidized azurin [eqn (2)]

$$\mathrm{Az(II)} + c\text{-551(II)} \underset{k_{21}}{\overset{k_{12}}{\rightleftharpoons}} \mathrm{Az(I)} + c\text{-551(III)} \qquad (2)$$

was studied for the wild-type and mutant proteins at pH 7.0 and 25 °C both at equilibrium, by redox titrations of reduced *c*-551 with oxidized azurin [9], and under pre-steady-state conditions, by mixing excess oxidized azurin with reduced *c*-551. The equilibrium constants are reported in Table 2, together with the second-order rate constants k_{12} obtained from the data reported in Figure 3. Since the driving force of the reaction at this pH ($\Delta E_{m,7}$) is very similar for the wild-type protein and for the mutants, and since Trp^{56} is not a surface residue in *c*-551, any observed difference in ET rates should primarily be ascribed to a difference in the intramolecular ET caused by the mutation. Indeed, as shown in Table 2, the differences observed in the ET rates to azurin for both the wild-type and W56F or W56Y mutants are not significant.

Figure 4 Superimposition of MD average structure of W56F on X-ray-crystallographic structure of wild-type *c*-551

The backbone trace and haem group are shown for the wild-type (thick black line) and W56F (thin black line). The side chain of residue 56 is also shown for both proteins.

MD characterization of wild-type and mutant *c*-551

An MD investigation was carried out on the wild-type and mutant simulated structures in order to evaluate potentially relevant differences. The following results were obtained for W56F: the 62–69 region moves towards the outside of the protein leading to a sliding of the haem parallel to its plane, and the His^{16}–iron bond is stretched; as a consequence, the His^{16}–Pro^{25} hydrogen bond is lost and the mobility of the 19–25 region increases (hence the haem pocket breathing is wider in this case); the average distance of the loop 53–59 from the haem increases by 0.7 Å in comparison with the native protein. The comparison between the wild-type X-ray-crystallographic structure and the simulated W56F mutant structure is shown in Figure 4; the aromatic rings of residues 56 overlap, and the whole loop and the strand including residue 61 are displaced. In the case of W56Y the simulated structure is much the same as the wild-type protein, except in the region of loop 53–59, where a slight movement towards the haem edge is observed, leading to the superimposition of the O of Tyr on the N^{ϵ} of Trp, with a difference of 0.3 Å in the average structures (not shown).

The relevance of the structural modifications after energy minimization and MD on the ET coupling calculations was evaluated in order to estimate the properties of the mutant cytochromes compared with the wild-type. The results of the GREENPATH program for the wild-type protein from X-ray crystallography were first compared with those obtained from the MD structure of the same protein. The same program was then used to evaluate the electronic coupling of W56F and W56Y mutants, the structures of which come from minimization of the MD average. In the native protein the major coupling between the iron and peptide chain involves the regions 12–17 and 56–58, i.e. stretches that include the axial ligands. Also sequences 37–41 and 54–57 appear to be relevant to the ET in the native protein,

although the order of magnitude lowers from 10^{-1} to 10^{-5}. These coupling values decrease by a factor of two in MD-derived structures, since the above stretches are mobile and flexible and can move away from the iron. In the case of the W56F mutant, the coupling to the iron is less in the 53–57 loop than in the native protein; this is due to the loss of a hydrogen bond. The average values for this part of the mutant are half those of the native protein; this difference, however, is of the same order of magnitude as the decrease in coupling that was ascribed to flexibility and mobility. No relevant change is expected from these calculations in the ET properties for W56F and W56Y mutants, although the mutations presumably perturb the hydrogen-bond network of the haem pocket and affect its overall flexibility and mobility.

DISCUSSION

Heterologous expression of *c* cytochromes in *E. coli* proved to be difficult, perhaps as a consequence of the intrinsic low efficiency of *c* haem insertion by thioether bond formation in this organism. Few *c*-type cytochromes have been produced in the *E. coli* periplasm, and mostly under partially anaerobic growth conditions [37,38]. More recently, *Paracoccus denitrificans* has been used as a host for both cytoplasmic and periplasmic expression [39].

We have been able to express *Ps. aeruginosa* *c*-551 in the heterologous system of *Ps. putida*; this strictly aerobic species was chosen because it produces endogenous *c*-type cytochromes [40], and because it was successfully employed in the expression of the *c*-haem-containing *Ps. aeruginosa* nitrite reductase [21]. Recently, an alternative system for homologous expression of *c*-551 in a *Ps. aeruginosa* mutant strain has been reported [41]; these authors, however, did not report data on the characterization of the recombinant protein, and estimates of protein expression were based only on difference spectra of whole-cell extracts. The yield of *c*-551 from *Ps. putida* is rather high for a *c*-type cytochrome, and growth conditions are easy (aerobiosis) and economic, since the inducer is inexpensive and no precursor of the protoporphyrin IX, such as δ-aminolaevulinic acid, is necessary to achieve high-level expression, in contrast with other haem proteins. The protein, encoded by a signal-peptide-containing gene, is correctly exported to the periplasm and matured by the host endogenous proteases, as shown by the N-terminal sequence and M_r determination. This expression system (M. C. Silvestrini, F. Cutruzzolà, I. Ciabatti and E. Zennaro, Italian Patent no. A26501 Rs/mg) seems well suited for the high-level expression of bacterial *c*-type cytochromes and could find more general applications, for instance for eukaryotic cytochromes.

A thorough spectroscopic characterization (optical and CD spectra in the full range of interest), and determination of ET kinetics to oxidized azurin and of the redox potential as a function of pH show that the recombinant protein is indistinguishable from the native *c*-551 from *Ps. aeruginosa*.

Two site-directed mutants in which the Trp in position 56 was replaced with Phe and Tyr were prepared and expressed. The general optical and CD properties of both mutants are almost identical with those of the wild-type, except for the optical spectrum in the region of the aromatics, where a difference consistent with the Trp → Phe or Tyr substitutions was observed. These results suggest that no major changes in the three-dimensional structure are induced by mutation of Trp^{56}, and in particular that co-ordination of the haem is unperturbed.

ET to oxidized azurin at pH 7.0, measured for both wild-type and mutant *c*-551, shows that the equilibrium and second-order rate constants are very similar, and the observed differences (less than 1.5-fold) are not significant, since they are comparable with those seen between wild-type recombinant and *Ps. aeruginosa* *c*-551. Previous work from this and other groups showed that mutations on the surface of both azurin and *c*-551 affect the ET kinetics to a much larger degree (one to two orders of magnitude) ([42]; F. Cutruzzolà, M. Arese and M. C. Silvestrini, unpublished work). Residue 56 is not directly involved in the recognition of azurin, which is consistent with previous observations suggesting that the productive complex between azurin and *c*-551 is mainly driven by interaction of the hydrophobic patches present at the surface of both proteins [42]. These kinetic results provide experimental support for the finding, obtained by GREENPATH calculations, that no significant perturbation of the electronic coupling is observed on mutation of Trp^{56}.

The p*K* of the alkaline transition at 695 nm, diagnostic of the stability of the Met–Fe bond in oxidized *c*-551, is essentially unmodified in the W56Y mutant, whereas it is much lower (by 1.4–1.6 pH units) in W56F. Thus, in the latter mutant, the strength of the Met–Fe bond seems to be significantly decreased in comparison with the wild-type and W56Y proteins. A hint as to the structural interpretation of this behaviour comes from the results of the MD computations carried out on the wild-type and W56F simulated structure; in the mutant a displacement of the loop containing Met^{61} and a loss of the hydrogen bond between the axial ligand His^{16} and Pro^{25} were observed. The importance of hydrogen bonds and polar environment for the haem Fe(III)–methionine co-ordination has previously emerged for eukaryotic *c* cytochromes from mutagenesis at the haem periphery [43,44].

As previously outlined, in wild-type *c*-551, Trp^{56} is involved in a hydrogen-bonding network around HP-17, the ionization of which was related to the pH-dependence of redox potential. When Trp^{56} is replaced by Phe (but not Tyr) significant differences from wild-type were shown to occur, such as a marked increase in pK_{red} and a large decrease in the absolute value of the midpoint potential at high pH. We believe that side-chain hydrophobicity is not responsible for the observed behaviour, since similar p*K* values were measured for *c*-551 bearing either Trp or Tyr at position 56 (in spite of the decrease in hydrophobicity in going from Trp to Phe and to Tyr [45]). Relevant information on the propionate environment comes from the ionic-strength-dependence of the pK_{red551} (Table 1) which is present in the mutants but not in the wild-type, and is largest for W56F. In the latter mutant the HP-17 negative charge seems therefore to be partly compensated for by the increase in ionic strength [46], thus leading to a lower pK_{red551} under these conditions. This effect suggests that in this bacterial cytochrome the substitution of Trp^{56} with a residue of smaller size (Phe or Tyr) leads to increased solvent accessibility, which in the case of Tyr could be partly shielded by hydrogen-bonding to HP-17; interestingly, in the eukaryotic cytochrome *c* the pocket entrance is restricted by a protein loop, which is absent in *c*-551 [1]. The loss of hydrogen-bonding capability may also explain the pH-dependence of the W56F mutant. Previous NMR studies on HP-17 ionization p*K* are somewhat controversial: whereas Leitch et al. [18] assigned a pK_{red} of 7.2 and 8.2 to HP-17 carboxylate in *Ps. aeruginosa* and *Ps. stutzeri* respectively, more recently Cai and Timkovich [19] have shown that in *Ps. stutzeri*, where residue 47 is a His, this carboxylate ionizes with a p*K* of 3.0, whereas in *Ps. aeruginosa* *c*-551, bearing Arg^{47}, the same group has a p*K* of 7.2. The latter authors suggest that the different strength of the hydrogen-bond involving HP-17 and residue 47 (either His or Arg) controls the deprotonation of HP-17 carboxylate; however, they also emphasize that this event is not easily correlated with the pH-dependence of midpoint potential in the two proteins. Our results show that the pK_{red} is significantly

higher (10.4) in the W56F mutant, where no hydrogen bond should be formed to the HP-17 carboxylate; in contrast, almost no difference is observed for W56Y, where the hydrogen bond should be conserved. In view of our data, it should be concluded that, if the pK_{red} reflects the HP-17 ionization, a value of 10.4 should be assigned to this carboxylate in the W56F mutant; this seems a rather unlikely value for an acidic group and therefore suggests some alternative. On the other hand, the substantial decrease in the absolute value of the midpoint potential observed for W56F (see Figure 2) could be explained assuming that the deprotonated state of the HP-17 carboxylate is favoured in the absence of the second hydrogen bond, leading to a preferential stabilization of the Fe(III) state, and thus to a lower oxidation potential value at high pH.

In conclusion, we suggest that in W56F, HP-17 is deprotonated and bears a higher net negative charge than wild-type at neutral and alkaline pH, mainly as a consequence of the disruption of the hydrogen-bonding network around HP-17; this different charge distribution may influence (lower) the pK of Arg^{47}, which in the mutant W56F may control the pH-dependence of the redox potential. A clearer picture of the haem surroundings will require structural determination of both mutants by either NMR or X-ray diffraction; attempts to obtain crystals of the W56 mutants are currently in progress in our laboratory.

We believe that in bacterial *c*-551 (or structurally related molecules), in the absence of the protein loop surrounding the haem crevice, the Trp residue at position 56, located at the entrance of the haem pocket, plays the dual role of bulk hydrophobic centre and hydrogen-bond donor, the latter being important in the modulation of the redox properties of these *c* cytochromes. Indeed, all these proteins display pH-dependent redox properties and also much higher rates of electron self-exchange [1].

The conclusion reached in this work on the role of hydrogen-bonding at the haem periphery is somewhat different from that drawn from studies on other class-I *c* cytochromes (*S. cerevisiae* iso-1-cytochrome *c* and *Rh. caspulatus* cytochrome c_2). In these proteins, all of which bear a loop around the haem, the conserved Trp residue located near the haem propionate plays a key role as a hydrophobic core, but its hydrogen-bonding capability appears to be less important [47,48].

This work was completed within a PNR (Programma Nazionale di Ricerca) contract assigned from MURST to Pharmacia s.p.a. I.C., G.R., S.F., M.A. and A.A. are recipients of Pharmacia contracts. We are indebted to Dr. M. E. Schininà (University of Rome La Sapienza) for N-terminal sequences and to Dr. G. Orsini (Pharmacia-Farmitalia Carlo Erba, Nerviano, Milan, Italy) for MS determinations. A special acknowledgement goes to Mr. B. Volpi and Dr. M. Tomasi (Istituto Superiore di Sanità, Rome, Italy) for invaluable help with fermentation of bacterial strains. We thank Professor M. Brunori (University of Rome La Sapienza) for advice and suggestions during this work.

REFERENCES

1 Moore, G. R. and Pettigrew, G. W. (1990) Cytochromes *c*: Evolutionary, Structural and Physicochemical Aspects, Springer-Verlag, Berlin
2 Caffrey, M. S. (1994) Biochimie **76**, 622–630
3 Ambler, R. P. (1963) Biochem. J. **46**, 1289–1301
4 Horio, T., Higashi, T., Sasagawa, M., Kusai, K., Nakai, M. and Okunuki, K. (1960) Biochem. J. **77**, 194–201
5 Matsuura, Y., Takano, T. and Dickerson, R. E. (1982) J. Mol. Biol. **156**, 389–409
6 Detlefsen, D. J., Thanabal, V., Pecoraro, V. L. and Wagner, G. (1991) Biochemistry **30**, 9040–9046
7 Wherland, S. and Gray, H. B. (1977) in Biological Aspects of Inorganic Chemistry (Addison, A. W., Cullen, W. R., Dolphin, D. and James, B. R., eds.), pp. 289–368, Wiley Interscience, New York and London
8 Wilson, M. T., Greenwood, C., Brunori, M. and Antonini, E. (1975) Biochem. J. **145**, 449–457
9 Silvestrini, M. C., Brunori, M., Wilson, M. T. and Darley-Usmar, V. (1981) J. Inorg. Biochem. **14**, 327–338
10 Morton, R. A., Overnell, J. and Harbury, H. (1970) J. Biol. Chem. **245**, 4653–4657
11 Silvestrini, M. C., Tordi, M. G., Colosimo, A., Antonini, E. and Brunori, M. (1982) Biochem. J. **203**, 445–451
12 Tordi, M. G., Silvestrini, M. C., Colosimo, A., Tuttobello, L. and Brunori, M. (1985) Biochem. J. **230**, 797–805
13 Marcus, R. A. and Sutin, N. (1985) Biochim. Biophys. Acta **811**, 265–322
14 Keller, R. M., Wuthrich, K. and Pecht, I. (1976) FEBS Lett. **70**, 180–184
15 Nordling, M., Young, S., Karlsson, B. G. and Lundberg, L. G. (1990) FEBS Lett. **259**, 230–232
16 Arai, H., Sanbongi, Y., Igarashi, Y. and Kodama, T. (1990) FEBS Lett. **261**, 196–198
17 Ambler, R. P., Meyer, T. E. and Kamen, M. D. (1979) Nature (London) **278**, 661–662
18 Leitch, F. A., Moore, G. R. and Pettigrew, G. W. (1984) Biochemistry **23**, 1831–1838
19 Cai, M. and Timkovich, R. (1992) FEBS Lett. **311**, 213–216
20 Silvestrini, M. C., Galeotti, C. L., Gervais, M., Schininà, E., Barra, D., Bossa, F. and Brunori, M. (1989) FEBS Lett. **254**, 33–38
21 Silverstrini, M. C., Cutruzzolà, F., D'Alessandro, R., Brunori, M., Fochesato, N. and Zennaro, E. (1992) Biochem. J. **285**, 661–666
22 Mermod, N., Ramos, J. L., Lehrbach, P. R. and Timmis, K. (1986) J. Bacteriol. **167**, 447–454
23 Mermod, N., Lehrbach, P. R., Donn, R. H. and Timmis, K. N. (1984) EMBO J. **3**, 2461–2466
24 Lederberg, E. M. and Cohen, S. N. (1974) J. Bacteriol. **119**, 1072–1074
25 Inouye, S. and Inouye, M. (1987) in Synthesis of DNA and RNA (Narang, S. A., ed.), pp. 181–206, Academic Press, New York
26 Parr, S. R., Barber, D., Greenwood, C., Phillips, B. W. and Melling, J. (1976) Biochem. J. **157**, 423–430
27 Schagger, H. and von Jagow, G. (1987) Anal. Biochem. **166**, 368–379
28 Thomas, P. E., Ryan, D. and Levin, W. (1976) Anal. Biochem. **75**, 168–176
29 Pettigrew, G. W., Meyer, T. E., Bartsch, R. G. and Kamen, M. D. (1975) Biochim. Biophys. Acta **430**, 197–208
30 Angelucci, L., De Gioia, L. and Fantucci, P. (1993) Gazz. Chim. Ital. **123**, 111
31 Regan, J. J., Rissr, S. M., Berathan, D. N. and Onuchic, J. N. (1993) J. Phys. Chem. **97**, 13083–13088
32 Skourtis, S. S., Berathan, D. N. and Onuchic, J. N. (1993) Chem. Phys. **176**, 501–503
33 Tordi, M. G., Silvestrini, M. C., Colosimo, A., Provencher, S. and Brunori, M. (1984) Biochem. J. **218**, 907–912
34 Moore, G. R., Pettigrew, G. W., Pitt, R. C. and Williams, R. J. P. (1980) Biochim. Biophys. Acta **590**, 261–271
35 Ferrer, J. C., Guillemette, J. G., Bogumil, R., Inglis, S. C., Smith, M. and Mauk, G. A. (1993) J. Am. Chem. Soc. **115**, 7507–7508
36 Senn, H., Keller, R. M. and Wutrich, K. (1980) Biochem. Biophys. Res. Commun. **92**, 1362–1369
37 Sambongi, Y., Yang, J. H., Igarashi, Y. and Kodama, T. (1991) Eur. J. Biochem. **198**, 7–12
38 Ubbink, M., Van Beeumen, J. and Canters, G. W. (1992) J. Bacteriol. **174**, 3707–3714
39 Sambongi, Y. and Ferguson, S. J. (1994) FEBS Lett. **340**, 213–216
40 Pettigrew, G. W. and Moore, G. R. (1987) Cytochromes *c*: Biological Aspects, Springer-Verlag, Berlin
41 Arai, H., Zhang, Y., Sanbongi, Y., Igarashi, Y. and Kodama, T. (1995) J. Ferment. Bioeng. **79**, 489–492
42 van de Kamp, M., Silvestrini, M. C., Brunori, M., van Beeumen, J., Hali, F. C. and Canters, G. W. (1991) Eur. J. Biochem. **194**, 109–118
43 Margoliash, E., Schejter, A., Koshy, T. H., Luntz, T. L. and Garber, E. A. E. (1990) in Bioenergetics (Kim, C. H. and Ozawa, T., eds.), pp. 125–145, Plenum Press, New York
44 Luntz, T. L., Schejter, A., Garber, E. A. E. and Margoliash, E. (1989) Proc. Natl. Acad. Sci. U.S.A. **86**, 3524–3528
45 Nozaki, Y. and Tanford, C. (1971) J. Biol. Chem. **246**, 2211–2217
46 Bertrand, P., Mbarky, O., Asso, M., Blanchard, L., Guerlesquin, F. and Tegoni, M. (1995) Biochemistry **34**, 11071–11079
47 Schweingruber, M. E., Stewart, J. W. and Sherman, F. (1979) J. Biol. Chem. **254**, 4132–4143
48 Caffrey, M. S. and Cusanovich, M. A. (1993) Arch. Biochem. Biophys. **304**, 205–208

Received 5 July 1996/1 October 1996; accepted 4 October 1996